Eighth Australasian Fluid Mechanics
Conference, University of Newcastle,
N.S.W., 28 November/2 December 1983.

THE STRUCTURE AND DYNAMICS OF OCEANIC TRANSIENT THERMOCLINES

J.W. HILL

RA.N. RESEARCH LABORATORY

DARLINGHURST, N.S.W. 2010 AUSTRALIA

SUMMARY

The topic of transient thermoclines, or temperature rises which develop at the top of the oceanic mixed layer on calm sunny days, is virtually untreated in the literature of physical oceanography. Here a data set is presented, and a well-known mixed layer model is rationally modified in order to secure useful fits. It is demonstrated that Ri approaches 1.0 at the bottom of the transient, connoting an intensity of stratification which is possibly unique in natural turbulence phenomena. It is inferred that turbulent kinetic energy storage, commonly ignored in the energy balance, may be important immediately beneath the transient.

1. INTRODUCTION

Transient thermoclines, often simply called transients, are temperature rises in the top 30 m or so of the nominally-isothermal oceanic mixed layer which can develop during the day under conditions of bright sunlight and low wind. They are becoming increasingly significant with the advent of sea surface temperature measurement by satellite. Moreover they are important to Defence authorities for their influence on the performance of some types of sonar. Because the temperature rise causes a rise in near-surface sound speed, its practical effect is to refract a sonar beam downwards; in consequence the beam can miss its target altogether except at unsatisfactorily low ranges.

The forcing influences are the entering heat flux (solar heating minus surface cooling) and horizontal momentum flux (wind stress), the same as govern mixed-layer behaviour generally. It is curious, then, that while much effort has been devoted to studying mixed layer behaviour, almost nothing analogous is to be found in the literature concerning transients. This is the more surprising in that transients represent the first contact of the forcing influences with the ocean medium, and in that they are comparatively easy to observe. The temperature profiles are readily accessible and large enough for accurate measurement. As they develop and disappear daily, a number may be observed during a single oceanographic cruise. In this paper two sets of diurnal temperature profiles are presented together with their meteorological forcing influences. A general description of transients is attempted. An empirical modelling approach is then developed, beginning with a well-known mixed layer model and adapting it to transients progressively as experience is gained with model fitting.

It is concluded that transients exhibit a degree of stratification which is possibly unique among natural turbulence phenomena. It is inferred, with less certainty, that in the region immediately beneath the transient, turbulent kinetic energy storage plays an important part in the overall energy balance.

2. AN OBSERVED DATA SET

In anticipation of the present studies a data set was acquired by the author during a research cruise by HMAS DIAMANTINA in the Indian Ocean during May 1976. Meteorological observations were made by trained ship's staff and temperature profiles were taken by Sippican expendable bathythermograph (XBT), all at two-hourly intervals over two consecutive days. Since the conditions for both were similar, all data is composited

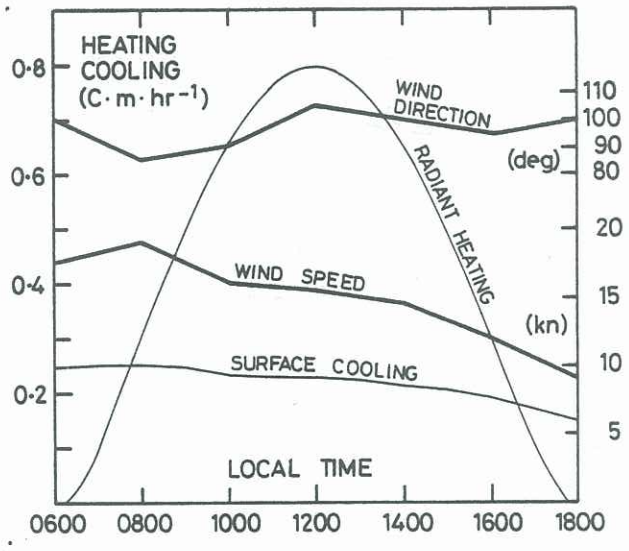

Figure 1. HMAS DIAMANTINA cruise May 4/5 1976, composited meteorological data.

in order to improve accuracy. Figure 1 shows the wind speed (U) and direction, also the penetrative radiant heating (Q) and surface cooling from all causes (S) calculated from the meteorological observations. The heat unit used, C·m, enters naturally when estimating water heat as the area under a profile scaled in $^{\circ}C$ and m : 1 C·m = 4.0 MJ m^{-2}. The later XBT profiles, digitized using simple magnification techniques and processed to improve smoothness, are shown in heavy line in Figure 3. Since XBT's are subject to a large error in absolute temperature ($0.2^{\circ}C$), a new baseline is fitted to each profile to make the included area equal to the cumulative net heating found from Figure 1. The near approach of the profiles to their baselines towards the bottom of the mixed layer gives confidence in this procedure. We see that the surface temperature rise reaches a maximum at time 1400 - 1600 and thereafter decreases; meanwhile the whole profile steadily deepens. Towards the end of the day the profile tends to develop an isothermal "front", clearly due to convective overturning as surface cooling overtakes radiant heating (Figure 1). The remainder of the profile becomes increasingly steep at the point of

inflexion, producing a characteristic overall appearance like the half-section view of a wineglass. At increasing depths, the increasing temperature gradient together with the necessarily decreasing heat transport connote a major reduction in turbulent diffusion, i.e. greatly increased stratification.

3. THE MELLOR AND DURBIN MODEL

We now attempt to model these transient profiles using the meteorological data of Figure 1 as input. Since very few complete data sets are currently available, the model must be simple with few means of adjustment. Accordingly we begin with the model of Mellor and Durbin (1975), henceforth MD, which as well as being simple is well-known and widely accepted. Indeed the present paper owes its title to that of the MD paper. Their model is now briefly recapitulated.

The downward transmission of heat and momentum are governed by conventional diffusion equations for temperature (T) and horizontal velocity ($\underset{\sim}{W}$)

$$\frac{\partial T}{\partial t} = \frac{\partial}{\partial z}\left(K_H \cdot \frac{\partial T}{\partial z}\right) + Q(t) \cdot DR(z) \qquad (1)$$

$$\frac{\partial \underset{\sim}{W}}{\partial t} = \frac{\partial}{\partial z}\left(K_M \frac{\partial \underset{\sim}{W}}{\partial z}\right) - (\underset{\sim}{k} \times \underset{\sim}{W})\, f. \qquad (2)$$

In (1) the radiant interception/depth relationship DR(z) is obtained from the data of Jerlov (1968, Table XXI), with the water assumed to be of optical classification Oceanic Ib. In (2), $\underset{\sim}{k}$ is the unit upward vector and f the Coriolis acceleration. The initial condition is a well-mixed layer with T = 0, $\underset{\sim}{W}$ = 0 throughout. The boundary conditions are: at the surface $K_H \frac{\partial T}{\partial z} = S(t)$, $K_M \frac{\partial \underset{\sim}{W}}{\partial z} = \underset{\sim}{\tau}_o(t)$;

and at the bottom of the mixed layer $K_H \frac{\partial T}{\partial z} = K_M \frac{\partial \underset{\sim}{W}}{\partial z} = 0$. The surface stress $|\underset{\sim}{\tau}_o|$ is found from the bulk aerodynamic formula

$$|\underset{\sim}{\tau}_o| = C_D \frac{\rho air}{\rho sea} U^2$$

with C_D, ρair and ρsea taken as .0013, .0012 and 1.02 respectively. With the thermal and mechanical diffusivities K_H and K_M assumed known, in a numerical solution (1) and (2) become sets of simultaneous linear equations which are processed by well-known computational techniques.

These equations are closed by formulations of K_H and K_M in terms of the bulk system variables, obtained as follows. In a one-dimensional model the standard turbulent kinetic energy (TKE,E) balance, with the storage and diffusion terms assumed small, is

$$\underset{\sim}{\tau} \cdot \frac{\partial \underset{\sim}{W}}{\partial z} - g\,\beta\,Q - \varepsilon = 0 \qquad (3)$$

whence it follows immediately that

$$\varepsilon = W_z^2(K_M - K_H\, Ri) \qquad (4)$$

with the velocity gradient $|\frac{\partial \underset{\sim}{W}}{\partial z}|$ written as W_z.

Using a rationale developed in related papers, e.g. Mellor and Yamada (1974), MD model ε, K_H and K_M by the formulations

$$\varepsilon = E^{3/2}/B_1\, L \qquad (5)$$

$$K_H = LE^{\frac{1}{2}}\, S_H(Ri) \qquad (6a)$$

$$K_M = LE^{\frac{1}{2}}\, S_M(Ri). \qquad (6b)$$

Here S_H and S_M are algebraic functions of R_f supplied by the MD rationale and shown graphically in Figure 2; they are also algebraic functions of Ri because of the relationship $S_H/S_M \equiv R_f/Ri$. L is a turbulence length-scale specified as the product αℓ, where ℓ is a measure of the depth of the turbulent structure (here the transient depth)

$$\ell = \int_0^{MLD} E^{\frac{1}{2}}\, z\, dz \Big/ \int_0^{MLD} E^{\frac{1}{2}}\, dz \qquad (7)$$

B_1 and α are constants, to which are assigned the values 15.0 and 0.1 respectively.

Equations (4), (5), (6a), (6b) and (7) are readily manipulated to give

$$\ell = \frac{\int_0^{MLD} W_z(S_M - S_H\, Ri)^{\frac{1}{2}}\, z\, dz}{\int_0^{MLD} W_z(S_M - S_H\, Ri)^{\frac{1}{2}}\, dz} \qquad (8)$$

$$K_H = \ell^2 W_z \cdot S_H(S_M - S_H\, Ri)^{\frac{1}{2}} \cdot \alpha^2 B_1^{\frac{1}{2}} \qquad (9a)$$

$$K_M = \ell^2 W_z \cdot S_M(S_M - S_H\, Ri)^{\frac{1}{2}} \cdot \alpha^2 B_1^{\frac{1}{2}} \qquad (9b)$$

so that K_H and K_M are found explicitly from the bulk system variables, avoiding the need for iteration mentioned by MD. The value of the constant $\alpha^2 B_1^{\frac{1}{2}}$ is $(0.1)^2 \times (15.0)^{\frac{1}{2}}$ or .039.

Equations (1), (2), (8), (9a) and (9b) are solved numerically in discrete time steps (here 5 minutes), (1) and (2) alternately with the other three.

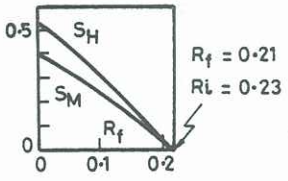

Figure 2. The functions $S_H(R_f)$, $S_M(R_f)$. After Mellor and Durbin (1975).

4. FIRST EXPERIENCES WITH FITTING THE MODEL

We now enter the data set of Figure 1 in the model. The modelled temperature profiles are added to Figure 3 in dotted line. Figure 4 shows the temperature and Ri profiles for time 1600 only in full line. We see that while the modelled temperature profiles are of the same general shape as the observed ones, they are too shallow and the surface temperatures too high. Higher values of K_H are clearly needed to reduce the temperature gradients, so referring again to (8a) we try increasing the numerical constant $\alpha^2 B_1^{\frac{1}{2}}$. The results obtained through increasing it by successive factors of 4 are added to Figure 4. We see that the temperature profile changes in the desired manner, but only to a limited extent. Meanwhile it becomes erratic, and the Ri results even more so. At the next increase of $\alpha^2 B_1$ (× 64) the computed solution is found to fail completely due to numerical overflow. We conclude that this type of model adjustment is unsuited to the present purpose, and accordingly look further afield.

5. THE LIMITATION ON Ri

The repeated encounters of Ri with its set limit of 0.23, seen in Figure 4, lead us to examine this feature of the MD model more closely. Referring again to (3), since

$$R_f \equiv g\,\beta\,Q/\underset{\sim}{\tau} \cdot \frac{\partial \underset{\sim}{W}}{\partial z}$$

is limited to 0.21 (Figure 2) we see that among the TKE terms

Production: buoyancy formation: dissipation =
1.0: 0.21 maximum: 0.79 minimum.

This limitation on stratification rests essentially upon observation of turbulent situations, e.g. Turner (1973). Transients, however, are relatively unstudied as yet, and clearly the observed ones of Figure 3 are highly stratified. Hence stratification may be more

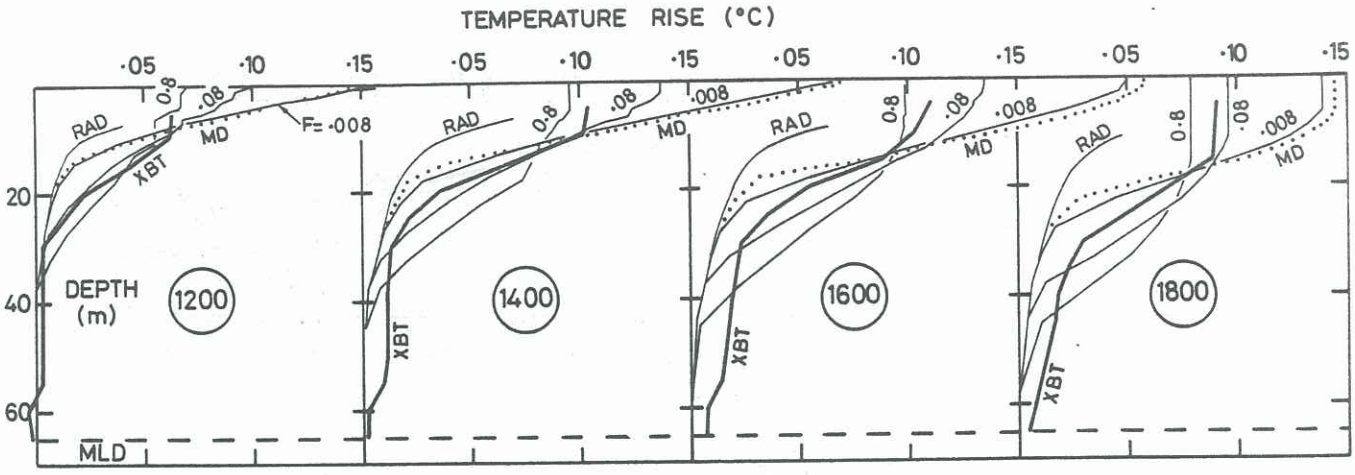

Figure 3. HMAS DIAMANTINA cruise May 4/5 1976. Observed (XBT) profiles and modelled profiles: Mellor and Durbin (MD, dotted line), new model (12) with F values as marked (full light line), radiant heating in the absence of diffusion (RAD, full light line).

important in transients than the above proportions would indicate. Accordingly we try removing the limitation. In the MD model it is applied through the functions S_H and S_M (Figure 2) so we replace these by constant factors. In thus departing from the MD rationale, we may as well drop the minor distinction which it makes between K_H and K_M, for the present at least. Thus we have $S_H = S_M = S$ (constant),

$K_H = K_M = K$, $R_f = Ri$. We find that (8), (9a) and (9b) reduce to

$$\ell = \int_0^{MLD} W_z(1 - Ri)^{\frac{1}{2}} z\, dz \Big/ \int_0^{MLD} W_z(1 - Ri)^{\frac{1}{2}}\, dz \quad (10)$$

$$K = \ell^2 W_z(1 - Ri)^{\frac{1}{2}} \cdot F \quad (11)$$

where F replaces the group $S^{3/2}\ \alpha^2\ B_1^{\frac{1}{2}}$ and is left undetermined for model fitting.

The formulation $K \propto L\, E^{\frac{1}{2}}$ which replaces (6a) and (6b) is a traditional one but is not universally endorsed. Bradshaw et al (1967) consider it a highly questionable assumption and in effect provide an alternative: the empirical approximation $E \doteq {}^{10}/_3 |\underline{\tau}|$. Combining this with (4) and (5) leads to

$$K = \ell^2 W_z(1 - Ri)^2 \cdot F \quad (12)$$

with F available as before for model fitting. In this case (7) becomes

$$\ell = \int_0^{MLD} (KW_z)^{\frac{1}{2}} z\, dz \Big/ \int_0^{MLD} (KW_z)^{\frac{1}{2}}\, dz. \quad (13)$$

6. FITTING THE NEW MODELS

The same data set as before is now entered in the new model (12), and the results are added to Figure 3 in light line. Here three values of F are used, viz .008, .08 and 0.8. The profiles produced by the central value give an uncritical best fit to the observed profiles. The other profiles are added to

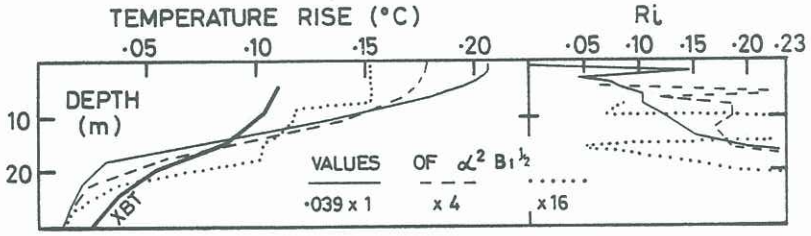

Figure 4. Observed and modelled results using MD model. Time 1600, conditions otherwise as for Figure 3. The constant $\alpha^2 B_1^{\frac{1}{2}}$ is increased by successive factors of 4.

show that such an optimum fit does exist.

Figure 5 shows the corresponding results for K and Ri. These are erratic in the top 10 m, but at greater depths show the progressive deepening of the transient more clearly than the temperature profiles do. We see that at any particular time K decreases with depth by 1 - 2 decades before finally falling to molecular level beneath the transient. Reverting to Figure 3, the profiles marked RAD show the temperatures that would result from the same radiant heating if turbulent diffusion were entirely absent. All of the modelled profiles collapse to the RAD profiles at sufficient depth, indicating complete stratification there. The K-profile for time 0800 is added to Figure 5 for comparison; this is just after radiant heating overcomes surface cooling (see again Figure 1), when convective overturning must cease.

We can now attempt a general description of transient dynamics: the well-mixed overnight layer persists so long as there is net cooling; thereupon a new turbulent regime commences to propagate downwards from the surface, at a rate governed by thermal and mechanical diffusion. The turbulence of the new regime is graded, being least at the bottom forefront where there had been stratification, and greatest near the surface where the forcing influences operate. The sub-transient region presents something of a paradox; we are forced to infer that it stratifies totally when the new regime begins (see again the 0800 K-profile), and only regains turbulence later in the day when the transient arrives; we shall have more to say about this in conclusion. We see that Ri increases with

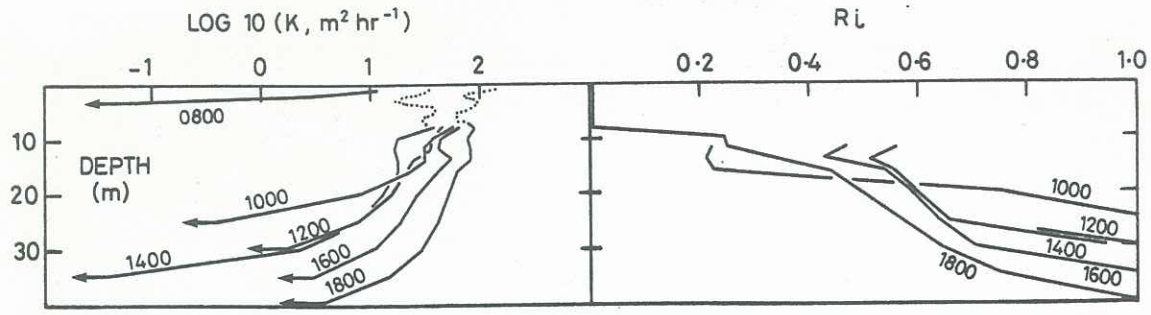

Figure 5. Results for K and Ri using new model (12). Time 1600, F = .08, conditions otherwise as for Figure 3. The arrowheads indicate a rapid fall of K to molecular level.

depth as K decreases, in accordance with (12), reaching 1.0 at the transient bottom. Hence we may conclude from (3) that turbulence dissipation falls to a level of unimportance at the bottom of the transient, and that the TKE balance there lies mainly between production and withdrawal to buoyancy. Such a degree of stratification in a natural turbulence phenomenon is possibly unique.

It remains to add that similar profiles are obtained with the new model (11) by setting F equal to .005, .05 and 0.5. These results differ from those of (12) only in being slightly more erratic. Since the two models differ only in their prescriptions for TKE dissipation, which we have found to be comparatively unimportant, such a similarity of outcome is to be expected.

7. CONCLUSION

The possibly unique nature of transients among natural turbulence phenomena has been indicated. Forming, as they do, an interface between the mixed layer and its forcing influences, they would seem to merit much more intensive study by physical oceanographers.

In closing we may consider the paradox of section 6 a little further: does the whole mixed layer really become totally stratified at the start of every sunny day? While instinct rebels, the observed temperature profiles of Figure 3 offer an accommodation. They appear to indicate heating at sub-transient depths (40 - 65 m) well in excess of the direct radiant heating (profiles RAD). Because of the method of baseline determination (section 2) such heating is by no means proved, although the developing gradient of the lower part of the profile appears to confirm it. If this heating is genuine it must be due to diffusion from above, indicating that turbulence is persisting from overnight at these depths. This would be in the absence of any new turbulence production and despite the stratifying influence of penetrative radiation. This can only mean that the storage term in the TKE balance is signficant, and cannot be ignored in the present situation as it so often is in more conventional turbulence modelling. A simple turbulence model which meets this requirement has already been presented (Hill, 1980). However this issue is beyond the scope of the present paper.

8. REFERENCES

BRADSHAW, P., FERRIS, D.H. and ATWELL, N.P. (1967). Calculation of boundary-layer development using the turbulent energy equation. J. Fluid Mech., 28, pp. 593-616.

HILL, J.W. (1980). Progress with modelling diurnal temperature profiles in the upper ocean. 7th Australasian Conference on Hydraulics and Fluid Mechanics, I.E. Aust. Nat. Conf. Pub. 80/4, pp. 381-384.

JERLOV, N.G. (1968). Optical Oceanography. Elsevier.

MELLOR, G.L. and DURBIN, P.A. (1975). The structure and dynamics of the ocean surface mixed layer. J. Phys. Oceanogr., 5, 718-728.

MELLOR, G.L. and YAMADA, T. (1974). A hierarchy of turbulence closure models for planetary boundary layers. J. Atmos. Sci., 31, pp. 1791-1806.

TURNER, J.S. (1973). Buoyancy effects in fluids. Cambridge University Press.